Measurement of Ocular Fundus Pulsation in Healthy Subjects Using a Novel Fourier-Domain Optical Coherence Tomography

Kanwarpal Singh,[1,2] *Carolyne Dion,*[1,2] *Marcelo Wajszilber,*[2] *Tsuneyuki Ozaki,*[1,2] *Mark R. Lesk,*[2,3] *and Santiago Costantino*[2,3,4]

Purpose. Anomalies in the pulsatility of the eye have been associated with many types of ocular pathology. Estimation of ocular pulsatility is usually obtained by measuring the variation in the intraocular pressure using tonometry-based instruments. In this work, the authors present and demonstrate the applicability of a novel and noninvasive Fourier-domain optical coherence tomography (FD-OCT) system to measure pulsatile ocular tissue movements.

Methods. The authors simultaneously measured the longitudinal movement of the cornea and the retina driven by the cardiac cycle in 21 healthy volunteers using their custom-made FD-OCT. They calculated the corresponding fundus pulse amplitude (FPA), which is the variation in the distance between the cornea and the retina.

Results. It was found that in young, healthy subjects, the cornea and the retina move axially during the cardiac cycle, with almost equal amplitude but with a phase difference ranging between 1° and 20°. The measured FPA was found to be mostly due to the relative phase difference between corneal and retinal movements, and frequency analysis revealed the presence of the harmonics of heartbeat. The root-mean-square values for cornea, retina, and FPA movements were found to be 28 ± 9 μm, 29 ± 9 μm, and 4 ± 2 μm, respectively. The dominant frequency component in corneal and retinal movement was found to be the second harmonic of the heartbeat.

Conclusions. The technique described here is useful for a precise description of FPA and the movement of ocular tissues. Further investigations and technical improvements will be beneficial for understanding the role of choroidal pulsation in the pathophysiology of ocular diseases. (*Invest Ophthalmol Vis Sci.* 2011;52:8927–8932) DOI:10.1167/iovs.11-7854

From the [1]Institut National de la Recherche Scientifique-Énergie, Matériaux et Télécommunications, Québec, Canada; the [2]Centre de Recherche de l'Hôpital Maisonneuve-Rosemont, Montréal, Québec, Canada; and the [3]Department of Ophthalmology, Faculty of Medicine, and [4]Biomedical Engineering Institute, Université de Montréal, Montréal, Québec, Canada.

Supported by the Ministère du Développement Économique de l'Innovation et de l'Exportation du Québec, the Fonds Québécois de la Recherchesur la Nature et les Technologies, the Canadian Institutes of Health Research, the Fonds de la Recherche en Santé du Québec, le Fonds de Recherche en Ophthalmologie de Universite de Montreal, the Natural Sciences and Engineering Research Council of Canada, and the Canadian Institute for Photonic Innovations.

Submitted for publication May 10, 2011; revised September 8, 2011; accepted September 20, 2011.

Disclosure: **K. Singh**, None; **C. Dion**, None; **M. Wajszilber**, None; **T. Ozaki**, None; **M.R. Lesk**, None; **S. Costantino**, None

Corresponding author: Santiago Costantino, Department of Ophthalmology, Faculty of Medicine, Université de Montréal, Montréal, Québec, H3T 1J4, Canada; santiago.costantino@umontreal.ca.

Several ocular pathologies—exudative age-related macular degeneration,[1] carotid artery stenosis,[2–4] normal tension glaucoma,[5,6] and giant cell arteritis[7]—have been associated with irregularities in the pulsatility of the eye. In addition, the relationship between the pulsatility of the eye and the incidence of glaucoma,[8] diabetes mellitus,[9] and central serous chorioretinopathy[10,11] have also been investigated. Ocular pulsatility has been attributed to the pulsatile nature of ocular hemodynamics.[12–14] Ocular hemodynamics plays an important role in the development of many ocular diseases, such as glaucoma,[15,16] age-related macular degeneration,[1] and diabetic retinopathy.[9] In addition, ocular pulsatility can be used to measure change in ocular volume,[17] based on which the rigidity of the eye can be calculated using the Friedenwald equation.[18] The estimation of ocular rigidity is important because it provides information about the biomechanical properties of the ocular tissues.

The imbalance between the pulsatile inflow and steady outflow of the blood causes a volume change in the eye. During inflow, the blood volume in the eye increases, causing an increase in intraocular pressure, which returns to its normal value during the outflow of the blood. Typically, ocular pulsatility is indirectly estimated by ocular pulse amplitude (OPA), defined as the difference between the minimum and the maximum intraocular pressure measured over the cardiac cycle. Tonometer-based technologies, such as pneumotonometry,[19,20] modified Goldmann applanation tonometry,[2] and dynamic contour tonometry,[21,22] are used to measure OPA. Nevertheless, because most techniques to assess ocular pulsatility actually measure pulsatile changes of IOP and require contact with the ocular surface, various alternative methods based on the measurement of longitudinal movements of ocular structures have been proposed. These methods measure a different aspect of the eye's response to pulsatile blood flow because they measure pulsatile anatomic changes rather than tonometric changes, and they may provide new insights into the physiology of sight and the pathophysiology of eye disease. Furthermore, they also have the advantage of not requiring contact with the eye.

The movements of the cornea and the retina are highly complex, with frequency components ranging from 1 to 150 Hz. The high-frequency movements, often called ocular microtremor, are associated with brain stem function,[23] whereas low-frequency movements are attributed to the pulsatile component of ocular blood flow.[12,13,24] It has been found that the longitudinal movement of the cornea is highly correlated with the cardiac cycle, as measured using ultrasonic transducers[3,25] and high-speed videokeratoscopy.[24,26] Although the transducers measure ultrasonic echoes to retrieve the movement of the cornea, videokeratoscopy uses the reflection of concentric rings projected on the cornea and analyzes its changes to evaluate the displacement. To assess fundus movement, differ-

ent technologies based on laser interferometry, such as low-coherence interferometry (LCI) and optical coherence tomography (OCT), have been used. Laser interferometry[27] uses a collimated laser beam of high coherence length to illuminate the eye, and the interference pattern resulting from the back-reflections of different ocular elements are recorded over time to extract the fundus pulse amplitude (FPA), which is the change in the distance between the cornea and the retina. For instance, the FPA has been used for studying ocular blood flow,[27,28] to estimate ocular rigidity,[17,29] and to study age-related macular degeneration.[30] However, because the coherence length of the lasers used in these studies was long, it was not possible to precisely determine which ocular elements produced the interference patterns obtained. To circumvent this problem and to measure the distance variations between two specific ocular elements, LCI was recently used.[29] Nevertheless, when using LCI, the information about the amplitude and direction of the movement of the individual ocular elements cannot be extracted. OCT has also been successfully applied to measure separately the movement of cornea, retina, and lens,[31] whereas Fourier-domain (FD) LCI has been shown in a rat model to be useful for measuring corneal and retinal displacement separately.[32]

In this study, we used a novel, noninvasive instrument based on FD-OCT to *simultaneously* measure the movement of the cornea and the retina at video rate (40 Hz). We tested our device on 21 healthy volunteers and obtained new information for characterizing the pulsatile ocular dynamics.

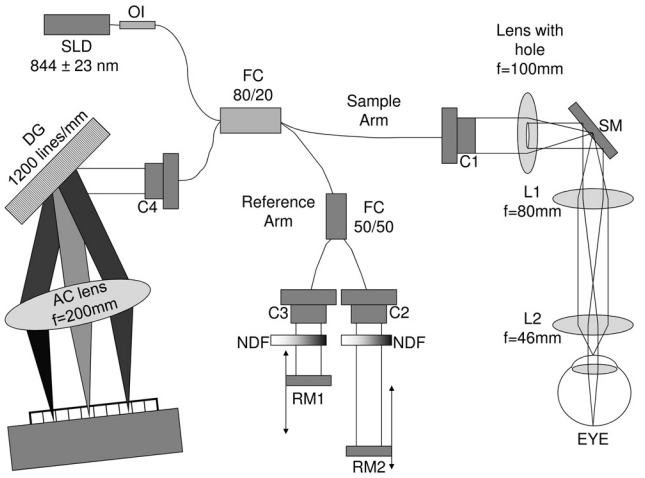

Figure 1. Schematic diagram of the optical system developed. An FT-OCT system, based on two reference arms and a holey focusing lens, allows simultaneous imaging of the cornea and the fundus at video rate. The hole in the lens enables scanning of the beam at the fundus at the macula position and a stationary laser spot at the corneal apex. The A-scans obtained combine positional information of both ocular elements. The components used in the system are superluminescent diode (SLD), optical isolator (IO), fiber couplers (FC), collimators (C1–C4), lenses (L) with focal length (f), reference mirrors (RM1-RM2), neutral density filter (NDF), scanning mirror (SM), dispersion grating (DG) and achromatic lens (AC).

Methods

Longitudinal movements of the retina at the macular region and of the corneal apex were simultaneously measured. In this study, 21 healthy volunteers (11 men, 10 women; age range, 25–35 years) were recruited. All the subjects had good cardiovascular health and no ocular pathologies other than myopia. The subject's head was placed on the head rest while the subject was asked to fixate on a target and blink normally. The eyes were not dilated before the procedure. These experiments were approved by the ethics committee of Maisonneuve-Rosemont Hospital, and the procedure adhered to the tenets of the Declaration of Helsinki. The procedure and its consequences were described to all the volunteers, and informed consent was obtained. Although previous studies have demonstrated that axial length and refractive error are major factors influencing ocular blood flow measurements,[33,34] for this study we did not collect such data because this was not a clinical trial.

Experimental Setup

A schematic diagram of the optical system used in this work is shown in Figure 1, in which a superluminescent diode (SLD; Superlum, Cork, Ireland) with 844-nm central wavelength and 46-nm bandwidth was coupled to a fiber-based Michelson interferometer. A 2 × 2, 80:20 fiber coupler was used to split the light into the reference and sample arms. The sample arm was terminated using a collimator that produced a 3-mm wide beam. The sample beam passed through a lens (f = 100 mm) with a central hole of 2 mm in diameter. After the lens, the central part of the sample beam remained collimated, but the outer part was refracted. A scanning system was set up so that the outer part of the sample beam was stationary and focused on the cornea, whereas the collimated central part was scanned and focused at the retina. Thus, using this optical scheme, we obtained simultaneously the reflected signals from the corneal apex and fundus at the macula region. A 2 × 1, 50:50 fiber coupler was used to obtain two reference signals reflected by mirrors mounted on separate motorized translation stages (Zaber Technology, Vancouver, BC, Canada). The reference signals were attenuated using neutral density filters to keep their total intensity below saturation level. The reflected signals from the sample and reference arms were dispersed using a reflective diffraction grating (1200 lines/mm) and were focused by an achromatic lens (f = 200 mm) on a linear charge-coupled device camera (Spyder 3; Dalsa Technology, Bromont, PQ, Canada).

A custom-made oximeter was placed on the ear lobe during measurements to simultaneously record the heartbeat of the subjects using a data acquisition card (Labjack, Lakewood, CO). The signals from the linear CCD camera and the oximeter were processed using a dual-core 2.0 GHz computer with custom software (LabView; National Instruments, Austin, TX). Data were acquired for 20 seconds and stored for later processing.

The bandwidth of the SLD used allowed a theoretical axial resolution[35] of approximately 7 μm in air. Setting the camera exposure time to 30 μs, the total frame rate (or B-scan rate) achieved was 40 frames per second. Each B-scan consisted of 720 A-scans with 1250 pixels per A-scan. For scanning, a 2D scanner (Nutfield Technology, Inc., Hudson, NH) was used, but only one mirror was moved to acquire the B-scans of the retina along a line. The maximum depth range of the system was found to be 3.26 mm in free space. The signal-to-noise ratio (SNR) of the system was 86 dB in the low-frequency range and 47 dB near 80% of the maximal-depth range, using a mirror as a sample and following the definition used in previous studies.[32] To calibrate the system, one reference mirror was moved in steps of 100 μm, and the corresponding FFT peak position was tracked.

In FD-OCT–based systems, the displacement resolution (i.e., the smallest position change that can be measured for a well-resolved peak) depends on the SNR of the system[36] and is basically limited by shot noise.[37,38] To experimentally estimate such displacement resolution of our system, a human cadaver eye was used as a sample. The eye was mounted on a piezoelectric stage (Piezosystem, Jena, Germany), which was moved sinusoidally with variable amplitude at 1 Hz. For filtering out the noise, frequencies lower than 0.75 Hz and higher than 5 Hz were removed. The piezoelectric stage was driven by a sine wave voltage and moved with amplitudes of 500 nm, 1 μm, and 2 μm. The SD of the noise, after subtracting the measured movement from the perfect sine wave fit, was approximately 100 nm.

Statistical Analysis

The fast Fourier transforms (FFT) of the recorded interferograms were computed to obtain axial scans (A-scans) containing positional information of both the cornea and the fundus. The positions of the corneal apex and the fundus at the macula were measured from sequential A-scans using the technique described in our previous work.[32] A detailed explanation of how data were processed is provided as Supplementary Material (http://www.iovs.org/lookup/suppl/doi:10.1167/iovs.11-7854/-/DCSupplemental). Briefly, A-scans were represented by the FFTs of the acquired interferograms, and the positions of the reflective interfaces identified in the sample were proportional to the locations of their corresponding FFT peaks. The accuracy of measuring movements of a sample strictly depends on the precision in locating the position of these FFT peaks; optimized accuracy can be achieved by locating the centroid of the FFT peak in the A-scans or by curve fitting.[32,39]

Finally, to retrieve the FPA, the difference between the positions of the cornea and the retina were calculated and further Fourier transformed to study their harmonic components compared with those of the cardiac cycle. Signals were processed by applying a bandpass frequency filter between the heartbeat and its fifth harmonic. For statistical data analysis, a paired *t*-test model was used, and $P < 0.05$ was considered statistically significant.

Results

A typical B-scan obtained with our system is shown in Figure 2, along with the A-scan at the visual axis. Comparison with available OCT images[35,40] enabled us to positively identify in the A-scans the corneal epithelium (CEp) and endothelium (CEn), the nerve fiber layer (NFL), the inner-outer segment (IS-OS), the retinal pigment epithelium (RPE), and the choriocapillaris (CC). From each B-scan, the position of the front surface of the cornea and an averaged position of the retina were located, and their displacement in time was traced. We

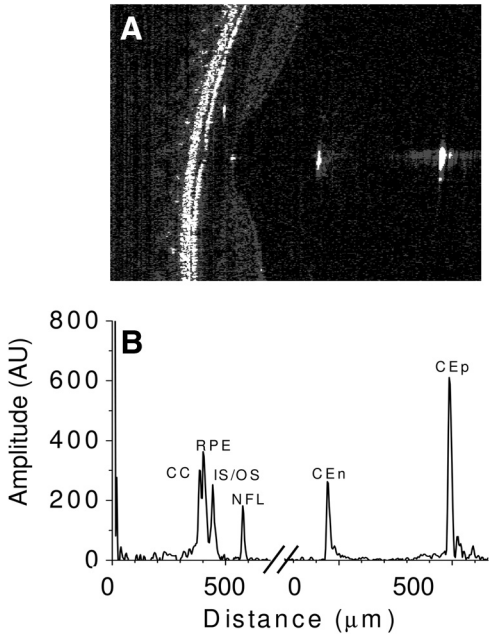

Figure 2. (**A**) Typical B-scan of the eye obtained with our system. The two reference arms were adjusted to bring the corneal and the retinal A-scans close together for analysis. (**B**) Different ocular structures at different depths of imaged tissue are identified in a single A-scan along the visual axis, as follows: corneal epithelium (CEp) and endothelium (CEn), nerve fiber layer (NFL), inner-outer segment (IS-OS), retinal pigment epithelium (RPE), and choriocapillaris (CC).

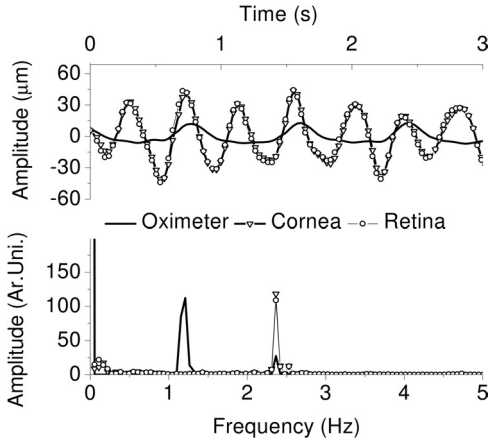

Figure 3. *Top*: the axial shift of the retina and the cornea along with oximeter signal in time. *Bottom*: Fourier transform showing the frequency components present in the retina and the cornea movement along with the frequency components of the oximeter signal. The peak to peak value of the axial sift is almost same for the cornea and the retina with a slight phase difference.

measured an averaged position of the retina, not the exact position of a particular layer because the reflected signal from a layer is more prone to noise over A-scans in time. In Figure 3, we show a fraction of one recording of the corneal and retinal movements, along with the oximeter signal measured in a 30-year-old man. The recording was made for 20 seconds, but for illustration purposes we show only the first 3 seconds of data.

To investigate the frequency components present in the movement, we show in the lower panel of Figure 3 the corresponding computed Fourier power spectrum. In Figure 4, we plot the difference between the corneal and retinal movements (i.e., the FPA) and the corresponding frequency analysis. Both Figure 3 and Figure 4 demonstrate the presence of harmonics in addition to the fundamental frequency of the heartbeat. It can also be observed in Figure 4 that FPA does not follow a perfectly regular pattern.

To validate this irregular pattern, we measured the FPA for 20 consecutive A-scans (covering approximately 100 μm). The FPA measured at each location was subtracted from the neighbor position, approximately 5 μm distant. Assuming that adjacent positions in the retina should exhibit equal FPA, the

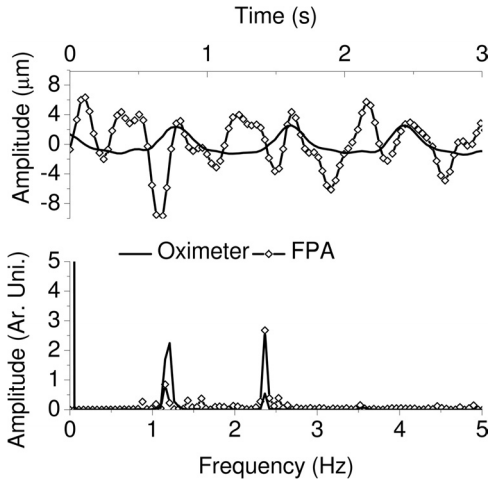

Figure 4. *Top*: FPA along with the oximeter signal. *Bottom*: frequency spectrum of the FPA and the oximeter signal.

difference obtained provides an estimate of the error in the measurement. The maximum measured peak-to-peak value of such difference in the FPA was 1.5 μm, and SD was 0.7 μm. These values, after applying a bandpass filter between 1 Hz and 5 Hz, are reduced to 1 μm and 0.3 μm, respectively. This filter minimizes errors in the measurement, induced by lateral and axial eye shifts caused by head movements[41] and microsaccades.[42] We also compared the movements at these 20 consecutive locations and found that the phase increased almost linearly with a phase difference of 1.4° between the 1st and the 20th A-scans analyzed (see Supplementary Fig. S1; http://www.iovs.org/lookup/suppl/doi:10.1167/iovs.11-7854/-/DCSupplemental).

We show in Figure 5 the frequency components that describe the movements of the cornea, the retina, and the FPA for all volunteers as box plots for the first four harmonics only. After applying a paired *t*-test, the distributions obtained showed significantly higher second harmonic components for both the retina ($P = 0.019$) and the cornea ($P = 0.015$) but a reduced contribution of this frequency for the FPA ($P = 0.707$).

Finally, we calculated the root-mean-square (RMS) for these movements, which represent the effective movement amplitude. For every measurement on a patient, at least 10 seconds of data were considered, corresponding to approximately 10 heart cycles. We computed the mean ± SD for the RMS of the cohort, yielding 28 ± 9 μm, 29 ± 9 μm, and 4 ± 2 μm for the cornea, retina, and FPA, respectively (Fig. 6A). In addition, in Figure 6B, we plotted the RMS value of the retinal movement with respect to the corneal movement for each volunteer. It was found that corneal and retinal movements were highly correlated with each other ($r = 0.99$). In all 21 subjects, after removing the data acquired during eye blinking, we could still analyze at least 10 cardiac cycles in each measurement. These results indicate that given the size of our sample, there was no significant difference ($P = 0.77$) between the amplitudes of the displacements of the cornea and the retina. Nevertheless, FPA can be measured by subtracting the absolute positions of the cornea and the retina.

The observation of FPA can be attributed to two facts: the difference between the amplitudes of the movement and the phase difference between the two movements (see Supplementary Fig. S2, http://www.iovs.org/lookup/suppl/doi:10.1167/iovs.11-7854/-/DCSupplemental, for an example in one volunteer). In our sample, the phase difference between corneal and macular movements varied between 1° and 20° for the fundamental frequency. Such measured phase difference between the two tissues for all the volunteers is shown in Supplementary Fig. S3 (http://www.iovs.org/lookup/suppl/doi:10.1167/iovs.11-7854/-/DCSupplemental) as box plots. We also calculated the phase difference up to the third harmonic of the heartbeat and obtained 7° ± 3°, 6° ± 4°, and 8° ± 4° for the fundamental, second, and third harmonics, respectively.

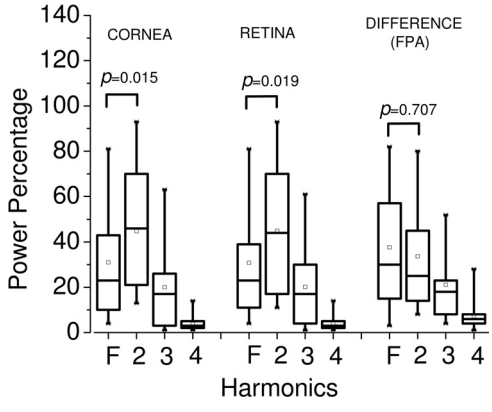

FIGURE 5. The movement of each ocular element was decomposed in frequencies, and the amplitudes corresponding to each harmonic were compared. The results show that the second harmonic of the cardiac pulsation is the principal frequency of both the corneal and the retinal movement. The *horizontal segments* in the boxes indicate 95th, 75th, 50th, 25th, and 5th percentiles (*top to bottom*), the *squares* inside the boxes represents the mean of the distribution, and the *stars* show the minima and maxima of the distributions.

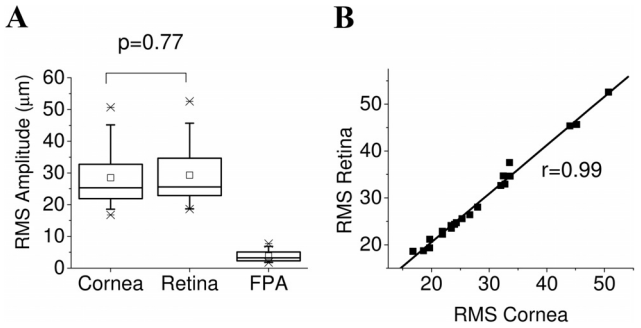

FIGURE 6. (**A**) RMS values of corneal, retinal, and FPA movements. The *horizontal segments* in the boxes indicate 95th, 75th, 50th, 25th, and 5th percentiles (*top to bottom*), the *squares* inside the boxes represent the mean of the distribution, and the *stars* show the minima and maxima of the distributions. (**B**) Corneal movement was plotted with respect to retinal movement for each volunteer to show the correlation between the two.

DISCUSSION

The system we developed could successfully measure the longitudinal movements of the cornea and the retina simultaneously with micrometer accuracy at video rates. To the best of our knowledge, the results we obtained with this system allow, for the first time and with a high degree of certainty, the conclusion that the cornea and the retina move with a small phase difference and almost equal amplitudes during the cardiac pulsations.

We were also able to monitor the corneal and retinal movements as well as the FPA, and were able to observe frequency components up to the seventh harmonic of the cardiac cycle (see Supplementary Fig. S4, http://www.iovs.org/lookup/suppl/doi:10.1167/iovs.11-7854/-/DCSupplemental). The dominant frequency component for both corneal and retinal movements was found to be the second harmonic, whereas there was almost equal contribution from the fundamental and second harmonic frequencies to the FPA. This is in agreement with the previous results of Kasprzak et al.,[31] in which the dominant frequency component was found to be the second harmonic of the heartbeat for both cornea and retina. A previous study[29] showed that the FPA occurs at the fundamental frequency of the heartbeat, but our results indicated that not only does the fundamental frequency contribute to the FPA but that other frequencies are also present and can be dominant.

Thus far, the mechanical properties of the ocular elements that move at harmonic frequencies of the heartbeat have not been addressed. Some related studies about the pulsatile blood flow measured in arteries close to the heart attributed the presence of frequency harmonics to tissue properties such as stiffness.[43–45] The technology we presented in this work provides a straightforward manner with which to characterize these movements and to build physical models that explain the dynamics observed in the eye. It will allow a better understanding of the mechanical forces that interact within the eye during the cardiac cycle and

their relevance to ocular pathology. For instance, our system can be used to study the eye length, which is of particular importance in myopia studies.[46] The FPA measured with our system could also help in the diagnosis of glaucoma[8,17,28] and age-related macular degeneration.[30] Furthermore, by tuning the wavelength of the laser source to improve penetration, our device could accurately describe the pulsatility of the choroid.

In conclusion, with a custom-designed FD-OCT system, we achieved, with high accuracy and for long periods of time, simultaneous measurement of corneal and the retinal positions, allowing for the first time a precise description of the eye's pulsatility. Briefly, during systole the expansion of the choroid pushes the retina forward, and the propagation of this pressure pulse reaches the cornea with a delay. The movements of the cornea and the retina are highly correlated ($r = 0.99$) with each other, and the amplitude of both tissues is almost equal, but a phase difference allows an FPA with RMS values of 4 ± 2 μm.

References

1. Mori F, Konno S, Hikichi T, Yamaguchi Y, Ishiko S, Yoshida A. Pulsatile ocular blood flow study: decreases in exudative age related macular degeneration. *Br J Ophthalmol.* 2001;85:531–533.
2. Perkins ES. The ocular pulse and intraocular pressure as a screening test for carotid artery stenosis. *Br J Ophthalmol.* 1985;69:676–680.
3. Zuckerman JL, Taylor KD, Grossman HJ. Noncontact detection of ocular pulse—correlation with carotid stenosis. *Invest Ophthalmol Vis Sci.* 1977;16:1018–1024.
4. McDonald PT, Rich NM, Collins GJJ, Kozloff L, Andersen CA. Ocular pneumoplethysmography: detection of carotid occlusive disease. *Ann Surg.* 1979;189:44–48.
5. Schwenn O, Troost R, Vogel A, Grus F, Beck S, Pfeiffer N. Ocular pulse amplitude in patients with open angle glaucoma, normal tension glaucoma, and ocular hypertension. *Br J Ophthalmol.* 2002;86:981–984.
6. Fontana L, Poinoosawmy D, Bunce CV, O'Brien C, Hitchings RA. Pulsatile ocular blood flow investigation in asymmetric normal tension glaucoma and normal subjects. *Br J Ophthalmol.* 1998;82:731–736.
7. Bosley TM, Savino PJ, Sergott RC, Eagle RC, Sandy R, Gee W. Ocular pneumoplethysmography can help in the diagnosis of giant-cell arteritis. *Arch Ophthalmol.* 1989;107:379–381.
8. Evans D, Hosking S, Embleton S, Morgan A, Bartlett J. Spectral content of the intraocular pressure pulse wave: glaucoma patients versus normal subjects. *Graefe's Archive Clin Exp Ophthalmol.* 2002;240:475–480.
9. Schmidt KG, von Rackmann A, Kemkes-Matthes B, Hammes H-P. Ocular pulse amplitude in diabetes mellitus. *Br J Ophthalmol* 2000;84:1282–1284.
10. Wang M, Munch IC, Hasler PW, Prünte C, Larsen M. Central serous chorioretinopathy. *Acta Ophthalmol.* 2008;86:126–145.
11. Tittl M, Polska E, Kircher K, et al. Topical fundus pulsation measurement in patients with active central serous chorioretinopathy. *Arch Ophthalmol.* 2003;121:975–978.
12. Silver DM, Farrell RA. Validity of pulsatile ocular blood flow measurements. *Surv Ophthalmol.* 1994;38(suppl):S72–S80.
13. Bosley T, Cohen M, Gee W, Reed J 3rd, Sergott R, Savino P. Amplitude of the ocular pneumoplethysmography waveform is correlated with cardiac output. *Stroke.* 1993;24:6–9.
14. Harris A, Kagemann L, Cioffi GA. Assessment of human ocular hemodynamics. *Surv Ophthalmol.* 1998;42:509–533.
15. Grieshaber MC, Mozaffarieh M, Flammer J. What is the link between vascular dysregulation and glaucoma? *Surv Ophthalmol.* 2007;52:S144–S154.
16. Harris A, Rechtman E, Siesky B, Jonescu-Cuypers C, McCranor L, Garzozi HJ. The role of optic nerve blood flow in the pathogenesis of glaucoma. *Ophthalmol Clin North Am.* 2005;18:345–353.
17. Hommer A, Fuchsjager-Mayrl G, Resch H, Vass C, Garhofer G, Schmetterer L. Estimation of ocular rigidity based on measurement of pulse amplitude using pneumotonometry and fundus pulse using laser interferometry in glaucoma. *Invest Ophthalmol Vis Sci.* 2008;49:4046–4050.
18. Friedenwald J. Contribution to the theory and practice of tonometry. *Am J Ophthalmol.* 1937;20:985–1024.
19. Silver DM, Farrell RA, Langham ME, O'Brien V, Schilder P. Estimation of pulsatile ocular blood flow from intraocular pressure. *Acta Ophthalmol.* 1989;67:25–29.
20. Langham ME, To'mey KF. A clinical procedure for the measurements of the ocular pulse-pressure relationship and the ophthalmic arterial pressure. *Exp Eye Res.* 1978;27:17–25.
21. Kniestedt C, Kanngiesser H. Dynamische Konturtonometrie. *Der Ophthalmologe.* 2006;103:713–723.
22. Punjabi OS, Kniestedt C, Stamper RL, Lin SC. Dynamic contour tonometry: principle and use. *Clin Exp Ophthalmol.* 2006;34:837–840.
23. Bolger C, Bojanic S, Sheahan NF, Coakley D, Malone JF. Dominant frequency content of ocular microtremor from normal subjects. *Vision Res.* 1999;39:1911–1915.
24. Kasprzak HT, Iskander DR. Spectral characteristics of longitudinal corneal apex velocities and their relation to the cardiopulmonary system. *Eye.* 2007;21:1212–1219.
25. Kowalska MA, Kasprzak HT, Iskander DR. Ultrasonic measurement of binocular longitudinal corneal apex movements and their correlation to cardiopulmonary system. *Biocybernet Biomed Eng.* 2008;28:35–43.
26. Kowalska MA, Kasprzak HT, Iskander DR. Comparison of high-speed videokeratoscopy and ultrasound distance sensing for measuring the longitudinal corneal apex movements. *Ophthalmic Physiol Opt.* 2009;29:227–234.
27. Schmetterer L, Dallinger S, Findl O, Eichler H-G, Wolzt M. A comparison between laser interferometric measurement of fundus pulsation and pneumotonometric measurement of pulsatile ocular blood flow 1. Baseline considerations. *Eye.* 2000;14:39–45.
28. Fuchsjager-Mayrl G, Wally B, Georgopoulos M, et al. Ocular blood flow and systemic blood pressure in patients with primary open-angle glaucoma and ocular hypertension. *Invest Ophthalmol Vis Sci.* 2004;45:834–839.
29. Dragostinoff N, Werkmeister RM, Groschl M, Schmetterer L. Depth-resolved measurement of ocular fundus pulsations by low-coherence tissue interferometry. *J Biomed Opt.* 2009;14:054047.
30. Schmetterer L, Kruger A, Findl O, Breiteneder H, Eichler H-G, Wolzt M. Topical fundus pulsation measurements in age-related macular degeneration. *Graefe's Arch Clin Exp Ophthalmol.* 1998;236:160–163.
31. Kasprzak H, Iskander DR, Bajraszewski T, Kowalczyk A, Nowak-Szczepanowska W. High accuracy measurement of spectral characteristics of movements of the eye elements. *Optica Pura Y Aplicada.* 2007;70:7–11.
32. Singh K, Dion C, Costantino S, Wajszilber M, Lesk MR, Ozaki T. Development of a novel instrument to measure the pulsatile movement of ocular tissues. *Exp Eye Res.* 2010;91:63–68.
33. James CB, Trew DR, Clark K, Smith SE. Factors influencing the ocular pulse—axial length. *Graefe's Arch Clin Exp Ophthalmol.* 1991;229:341–344.
34. Ravalico G, Pastori G, Croc, Egrave M, Toffoli G. Pulsatile ocular blood flow variations with axial length and refractive error. *Ophthalmologica.* 1997;211:271–273.
35. Wojtkowski M, Srinivasan VJ, Ko TH, Fujimoto JG, Kowalczyk A, Duker JS. Ultrahigh-resolution, high-speed, Fourier domain optical coherence tomography and methods for dispersion compensation. *Opt Expr.* 2004;12:2404–2422.
36. Singh K, Dion C, Lesk MR, Ozaki T, Costantino S. Spectral-domain phase microscopy with improved sensitivity using two-dimensional detector arrays. *Rev Scientific Instruments.* 2011;82:023706–023704.
37. Choma MA, Ellerbee AK, Yang C, Creazzo TL, Izatt JA. Spectral-domain phase microscopy. *Opt Lett.* 2005;30:1162–1164.

38. Zhang J, Rao B, Yu L, Chen Z. High-dynamic-range quantitative phase imaging with spectral domain phase microscopy. *Opt Lett.* 2009;34:3442–3444.
39. Costantino S, Martinez OE, Torga JR. Wide band interferometry for thickness measurement. *Opt Expr.* 2003;11:952–957.
40. Drexler W, Morgner U, Ghanta RK, Kartner FX, Schuman JS, Fujimoto JG. Ultrahigh-resolution ophthalmic optical coherence tomography. *Nat Med.* 2001;7:502–507.
41. Keshner FA, Peterson BW. Mechanisms controlling human head stabilization, I: head-neck dynamics during random rotations in the horizontal plane. *J Neurophysiol.* 1995;73:2293–2301.
42. Ricco S, Chen M, Ishikawa H, Wollstein G, Schuman J. Correcting motion artifacts in retinal spectral domain optical coherence tomography via image registration. In: Yang G-Z, Hawkes DJ, Rueckert D, Noble A, Taylor C, eds. *Medical Image Computing and Computer-Assisted Intervention—MICCAI 2009.* Heidelberg: Springer Verlag; 2009:100–107.
43. Nichols WW, Conti CR, Walker WE, Milnor WR. Input impedance of the systemic circulation in man. *Circ Res.* 1977;40:451–458.
44. Finkelstein SM, Collins VR, Cohn JN. Arterial vascular compliance response to vasodilators by Fourier and pulse contour analysis. *Hypertension.* 1988;12:380–387.
45. O'Rourke MF, Taylor MG. Input impedance of the systemic circulation. *Circ Res.* 1967;20:365–380.
46. Drexler W, Findl O, Schmetterer L, Hitzenberger CK, Fercher AF. Eye elongation during accommodation in humans: differences between emmetropes and myopes. *Invest Ophthalmol Vis Sci.* 1998; 39:2140–2147.